Tracing the Conversion Process from Primordial Germ Cells to Pluripotent Stem Cells in Mice 1

Authors: Nagamatsu, Go, Kosaka, Takeo, Saito, Shigeru, Takubo, Keiyo, Akiyama, Hideo, et al.

Source: Biology of Reproduction, 86(6)

Published By: Society for the Study of Reproduction

URL: https://doi.org/10.1095/biolreprod.111.096792

BIOLOGY OF REPRODUCTION (2012) **86**(6):182, 1–11
Published online before print 14 March 2012.
DOI 10.1095/biolreprod.111.096792

Tracing the Conversion Process from Primordial Germ Cells to Pluripotent Stem Cells in Mice[1]

Go Nagamatsu,[2,3,6] Takeo Kosaka,[3,5] Shigeru Saito,[7,8] Keiyo Takubo,[4] Hideo Akiyama,[9] Tetsuo Sudo,[9] Katsuhisa Horimoto,[7,10] Mototsugu Oya,[5] and Toshio Suda[4]

[4]*Department of Cell Differentiation, The Sakaguchi Laboratory, School of Medicine, Keio University, Tokyo, Japan*
[5]*Department of Urology, School of Medicine, Keio University, Tokyo, Japan*
[6]*Precursory Research for Embryonic Science and Technology (PRESTO), Japan Science and Technology Agency, Kawaguchi, Japan*
[7]*Computational Biology Research Center (CBRC), National Institute of Advanced Industrial Science and Technology (AIST), Tokyo, Japan*
[8]*Chem & Bio Informatics Department, INFOCOM Corporation, Tokyo, Japan*
[9]*Toray New Frontiers Research Laboratories, Kanagawa, Japan*
[10]*Institute of Systems Biology, Shanghai University, Shanghai, China*

ABSTRACT

To understand mechanisms underlying acquisition of pluripotency, it is critical to identify cells that can be converted to pluripotent stem cells. For this purpose, we focused on unipotent primordial germ cells (PGCs), which can be reprogrammed into pluripotent embryonic germ (EG) cells under defined conditions. Treatment of PGCs with combinations of signaling inhibitors, including inhibitors of MAP2K (MEK), GSK3B (GSK-3beta), and TGFB (TGFbeta) type 1 receptors, induced cells to enter a pluripotent state at a high frequency (12.1%) by Day 10 of culture. When we employed fluorescence-activated cell sorting to monitor conversion of candidate cells to a pluripotent state, we observed a cell cycle shift to S phase, indicating enrichment of pluripotent cells, during the early phase of EG formation. Transcriptome analysis revealed that PGCs retained expression of some pluripotent stem cell-associated genes, such as *Pou5f1* and *Sox2*, during EG cell formation. On the other hand, PGCs lost their germ lineage characteristics and acquired expression of pluripotent stem cell markers, such as *Klf4* and *Eras*. The overall gene expression profiles revealed by this system provide novel insight into how pluripotency is acquired in germ-committed cells.

acquisition of pluripotency, primordial germ cell, purification, tracing

INTRODUCTION

Somatic cells can be reprogrammed into pluripotent cells in vitro through introduction of four defined factors: *Pou5f1*, *Sox2*, *Klf4*, and *Myc* [1, 2]. Currently, it is possible to produce induced pluripotent stem (iPS) cells with characteristics identical to those of embryonic stem (ES) cells. This procedure is a major breakthrough in stem cell biology and has also been expected to be used for clinical applications in regenerative medicine. Several recent studies also report improved induction methods, including integration-free induction of reprogramming factors [3–9]. However, little is known about how cells alter their characteristics to those of pluripotent cells [10]. Although an understanding of reprogramming mechanisms is essential to manipulate iPS cells and iPS cell-derived differentiated cells, it is experimentally challenging to analyze changes occurring during the process due to a low frequency of conversion and the long culture periods required.

In vivo, germ cells only acquire totipotency after fertilization [11]. Germ cell development involves a sequence of reprogramming events, including drastic epigenetic changes [12]. Germ cells are specified from the epiblast at mouse Embryonic Day 7 (E7). At that time, primordial germ cells (PGCs) suppress the somatic program, including repression of genes of the *Hox* clusters; reactivate *Sox2*, which may function in the recapture of pluripotency potential; and commence genome-wide epigenetic reprogramming, including histone modification and DNA demethylation. In addition, an additional reprogramming process occurring in the embryonic gonad involves both erasure of imprinting and X chromosome reactivation [11]. Intriguingly, these germ cell specification processes are also related to somatic cell reprogramming [13]. Thus, an investigation of germ cell specification may provide useful clues to our understanding of somatic cell reprogramming.

Germ cells can be converted to pluripotent cells under appropriate culture conditions, as seen in the development of embryonic germ (EG) cells from PGCs and multipotent germline stem cells from spermatogonia [14, 15], both of which exemplify acquisition of pluripotency from unipotent germ lineages. The EG cell formation is more efficient and has a shorter culture period than somatic cell reprogramming, and it does not require exogenous genetic manipulations. Therefore, EG cell formation provides a good model to analyze mechanisms by which committed cells acquire pluripotency.

[1]Supported by PRESTO of the Japan Science and Technology Agency and Scientific Research (C) from MEXT (G.N.). This study was also supported in part by a grant from the Project for Realization of Regenerative Medicine, and support for the core institutes for iPS cell research was provided by MEXT, a Grant-in-Aid for the Global Century COE program from MEXT.
[2]Correspondence: Go Nagamatsu, Department of Cell Differentiation, The Sakaguchi Laboratory, School of Medicine, Keio University, 35 Shinano-machi, Shinjuku, Tokyo 160-8582, Japan.
E-mail: gonag@z2.keio.jp
[3]These authors contributed equally to this work.

Received: 7 October 2011.
First decision: 14 November 2011.
Accepted: 8 March 2012.

eISSN: 1529-7268 http://www.biolreprod.org
ISSN: 0006-3363

In this study, we developed an efficient culture method to produce EG cells from E11.5 PGCs using inhibitors of MAP2K (MEK), GSK3B (GSK-3β), and TGFB (TGF-β) type 1 receptor. Furthermore, we employed fluorescence-activated cell sorting (FACS) to purify pluripotent candidate cells during the culture period. Combining both techniques, we were able to enrich pluripotent candidate cells from PGCs at different time points and follow how germ cells acquire pluripotency. We observed significant changes in cell cycle status and expression patterns of the whole transcription by microarray.

MATERIALS AND METHODS

Mice

Nanog-GFP-IRES-puro transgenic mice (RBRC02290) were provided by RIKEN BRC, which participates in the National Bio-Resource Project of the Ministry of Education, Culture, Sports, Science and Technology (MEXT) of Japan. ICR and BALB/c nude mice were purchased from Japan SLC. Animal care was performed in accordance with guidelines established by Keio University (Tokyo, Japan) for animal use and recombinant DNA experiments. The PGCs were prepared by crossing *Nanog-GFP* with ICR mice.

Isolation and Culture of PGCs

Gonads from *Nanog-GFP-IRES-puro* transgenic embryos at E11.5 and E8.5 were dissociated to form a single-cell suspension by incubation with 0.05% trypsin and 0.02% ethylenediamine tetraacetic acid for 10 min. Suspensions were sorted by green fluorescent protein (GFP) fluorescence using a BD FACS AriaII cell sorter (BD Biosciences). Sorted PGCs were cultured on Sl/Sl^4-m220 or STO feeder cells with Knockout DMEM (Invitrogen) supplemented with 15% KnockOut Serum Replacement (KSR; Invitrogen), 2 mM glutamine, 1 mM nonessential amino acids, 2-mercapto-ethanol, leukemia inhibitory factor (LIF), and basic fibroblast growth factor (bFGF). All compounds were added from Day 1 until Day 7 of culture, except during the process of seeding on STO cells. When PGCs were seeded on STO cells, chemical compounds were added at the beginning of the culture. At Day 7, bFGF was removed by changing to fresh medium lacking bFGF. In the case of seeding on Sl/Sl^4-m220 cells, cells were collected and reseeded onto STO feeder cells on Culture Day 3.

Feeder Cell Preparation

Sl/Sl^4-m220 cells were treated with 5 μg/ml mitomycin C for 1 h and plated at a density of 4×10^5 cells per well in 24-well plates 1 day before use. STO cells were treated with 12 μg/ml mitomycin C for 2 h and plated at a density of 1×10^6 cells per 55 cm^2.

Chemical Compounds

The chemical compounds purchased for this study were trichostatin A (TSA; Sigma), valproic acid (VPA; Sigma), BIX (Alexis Biochemicals), 5-azacytidine (5AZA; Sigma), A83-01 (Sigma), and dorsomorphin (Sigma). Drs. S. Nishiyama, H. Okano, and W. Akamatsu (Keio University) kindly donated the inhibitors PD173074, PD325901, and CHIR99021, which were prepared by organic synthesis. The concentrations of compounds were TSA (1 ng/ml, 5 ng/ml), VPA (0.2 mM, 1.0 mM), BIX (0.1 μM, 0.5 μM), 5AZA (0.2 μM, 1 μM), A83-01 (25 nM, 250 nM), dorsomorphin (0.2 μM, 2 μM), PD173074 (10 nM, 100 nM), PD325901 (0.1 μM, 1 μM), and CHIR99021 (0.3 μM, 3 μM). For the combined use of PD325901, CHIR99021, and A83-01 (2i + A83), the concentrations were 1 μM PD325901, 3 μM CHIR99021 and 250 nM A83-01.

Antibodies and Flow Cytometry

Cultured PGCs were harvested in 0.05% trypsin. After washing, cells were incubated with anti-FcγR (FCER1G) antibody (2.4G2; eBioscience) at 4°C for 30 min. Then, cells were simultaneously incubated with APC-conjugated anti-SSEA-1 mAb (MC-480) (BioLegend) for 30 min at 4°C. Antibodies were used at 0.2 μg per 1×10^6 cells. After washing, samples were analyzed and sorted using the FACSAria II cell sorter (BD Biosciences). For cell cycle analysis, stained samples were fixed by 4% paraformaldehyde (PFA) and treated with 0.005% saponin (Sigma), 0.25 mg/ml RNase A, and 50 μg/ml propidium iodide (Molecular Probes) for 20 min at 37°C. Then, a BD FACSCalibur flow cytometer (BD Biosciences) was used to analyze the cells.

Microarray Data Analysis

A significant number of PGCs, pluripotent candidate cells at Days 3 and 6 of culture, and EG cells were collected by FACS purification. Expression profiles were analyzed using the 3D-Gene Mouse Oligo chip 24K (Toray Industries). Fluorescence intensities were detected using the Scan-Array Life Scanner (Perkin-Elmer), and PMT levels were adjusted to achieve 0.1%–0.5% pixel saturation. Each TIFF image was analyzed with GenePix Pro version 6.0 software (Molecular Devices). We made biological replicates and used average value. The data were filtered to remove low-confidence measurements and were globally normalized per array, such that the median of the signal intensity was adjusted to 50 after normalization (accession number GSE37261). Similarities of whole-gene expression profiles in four arrays were measured by Pearson correlation coefficients. Hierarchical sample clustering was performed by UPGMA method with Pearson correlation distance, and the whole genes were manually sorted based on their maximum expression values; the expression values were displayed as normalized values (i.e., the log2 gene expression value divided by the median). Furthermore, we designed the following procedure to perform the gene set enrichment analysis for the present case without any replicates. First, a gene list that sorted in the descending order based on fold-change between the PGCs, Day 3 (2i + A83) cells, Day 6 (2i + A83) cells, and EG (2i + A83) cells was calculated. Secondly, preranked gene set enrichment analysis was applied for the gene list to the manually curated gene sets for pluripotent and germ cell markers with default parameters (http://www.broadinstitute.org/gsea/index.jsp).

Alkaline Phosphatase Staining

The ES cells were fixed in 4% PFA/PBS for 10 min at 4°C, washed twice with PBS, and then stained using SCIP/NBT liquid substrate (B-1911; Sigma) for 30 min at 37°C.

Teratoma Formation

To produce teratomas, 1.0×10^6 cells were suspended in BD Matrigel (BD Biosciences) and injected into nude mice. Three to four weeks later, tumors were fixed with 4% PFA in PBS, embedded in paraffin, sectioned, and stained with hematoxylin and eosin.

Bisulfite Sequencing

Bisulfite reactions were performed with the EpiTect Bisulfite kit (Qiagen) according to the manufacturer's instructions. Primers used for PCR were described previously [16]. The PCR products were cloned into pGEM-T-easy (Promega) and sequenced by conventional means.

Time-Lapse Bioimaging

Cells were harvested on Culture Day 3, reseeded on STO feeder cells, and cultured overnight. Cells were analyzed using an LCV110 incubator microscope system (Olympus) and incubated at 37°C in 5% CO_2 during experiments. MetaMorph software (Universal Imaging) was used for image analysis.

RESULTS

Highly Efficient Induction of Pluripotent Stem Cells from PGCs

The PGCs were collected from E11.5 mouse embryos and cultured on S1/S1^4-m220 feeder cells in the presence of bFGF and LIF. After 10 days of culture, *Nanog-GFP*-positive colonies were counted [17]. Primordial germ cells undergo changes in characteristics such as proliferative capacity during various developmental stages. When they enter the embryonic gonad, PGCs undergo cell cycle arrest, making it difficult to generate EG cells at that time point. Here, because PGCs were obtained at E11.5 immediately prior to cessation of proliferation (Supplemental Fig. S1; all supplemental data are available online at www.biolreprod.org), the rate of conversion of PGCs to EG cells remained low, making it difficult to conduct a prospective analysis. Therefore, we aimed to develop a more efficient induction method.

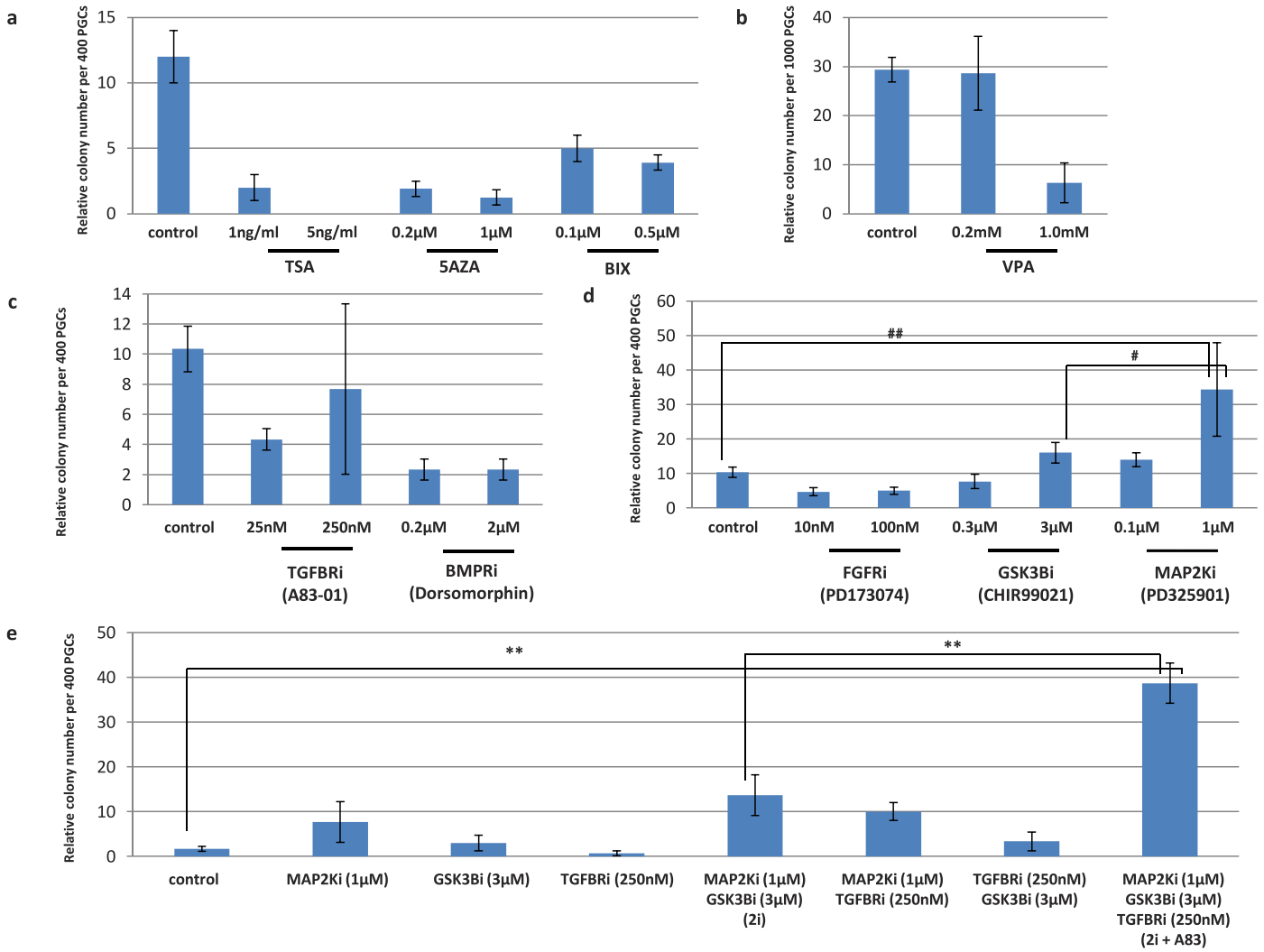

FIG. 1. Establishment of highly efficient culture conditions for EG cell formation. Chemical compounds promoting epigenetic modification (TSA, 5AZA, BIX-01294, and VPA) were screened for capacity to enhance EG cell formation (**a** and **b**). Each chemical was added at the indicated concentrations 1 day after cells were seeded. *Nanog-GFP*-positive colonies were counted on Day 10. **c** and **d**) Analysis of signaling inhibitors. $\#P = 0.0136$, $\#\#P = 0.0014$. Effects of the TGFB type 1R (A83-01) inhibitor or BMP type 1R inhibitor (dorsomorphin) are shown in **c**, whereas effects of the FGFR inhibitor (PD173074), the GSK3B inhibitor (CHIR99021), or the MAP2K inhibitor (PD325901) on EG cell formation are shown in **d**. The effects of different combinations of these inhibitors are shown in **e**. Each chemical except for those shown in **e**, was added at the concentrations indicated 1 day after the culture was seeded. For the chemicals in **e**, the concentration of each inhibitor was: MAP2K inhibitor (3 μM), the GSK3B inhibitor (1 μM), and the TGF-β type 1R inhibitor (25 mM). *Nanog-GFP*-positive colonies were counted on Day 10. $**P < 0.001$. All of the culture conditions contained LIF. Error bars indicate SD.

We first asked whether epigenetic modifications altered reprogramming efficiency. To do so, we undertook experiments employing histone deacetylase inhibitors TSA and VPA, the DNA demethylator 5AZA, and BIX-01294, a diazepinylquinazolinamine derivative with a specific inhibitory effect on G9a as an H3K9-specific methyl transferase, all of which reportedly increase reprogramming efficiency in nuclear transfer and/or induction of iPS cells [9, 18–20]. Each compound was applied to PGCs 1 day after seeding because we did not observe changes in efficiency when chemicals were applied immediately after culture initiation (data not shown). Although several colonies per hundred PGCs were observed in untreated control cultures, all of these small-molecule compounds decreased colony growth dose dependently following application, indicating an inhibitory effect (Fig. 1, a and b). These epigenetic alterations are not critical for EG cell formation from PGCs.

Induction of iPS cells from rat liver progenitors and human fibroblasts is reportedly enhanced by treatment of cells with small-molecule inhibitors, including inhibitors of MAP2K, GSK3B, and TGFB type 1R [21]. Embryonic stem cells can also be maintained without feeder cells, LIF, or serum in the presence of a combination of signaling inhibitors [22]. Such inhibitors include the MAP2K inhibitor PD325901, the GSK3B inhibitor CHIR99021, and the FGF receptor (FGFR) inhibitor PD173074. Significantly, combining two inhibitors (2i) PD325901 (for MAP2K) and CHIR99021 (for GSK3B) is reportedly particularly potent and allows cultured ES cells to remain in a self-renewal ground state [23]. Thus, we investigated the role of these signaling pathways during EG cell formation. The TGFB signaling and BMP signaling exert their effects via SMAD signaling. The addition of either a TGFB type 1R inhibitor (A83-01) or dorsomorphin, which inhibits BMP type 1R, had no effect (Fig. 1c). On the other hand, we found that PGCs cultured with the MAP2K inhibitor or the GSK3B inhibitor showed increased colony numbers, whereas addition of the FGFR inhibitor PD173074 had an inhibitory effect (Fig. 1d). The inhibitory effect of the FGFR

inhibitor for EG cell formation supports the idea that FGF signaling positively regulates EG cell formation [24]. Treatment of the MAP2K inhibitor and the GSK3B inhibitor showed additive effect (Fig. 1e). Furthermore, combining the MAP2K inhibitor and the GSK3B inhibitor (2i) with the TGFB type 1R inhibitor A83-01 produced a significant increase in EG colony formation (Fig. 1e). Although 2i was originally used in a serum-free condition [22], we refer to the combination of MAP2K inhibitor and the GSK3B inhibitor in the culture containing KSR as 2i in this paper.

Because *Nanog-GFP*-positive cells in colonies generated in the presence of bFGF + 2i + A83 proliferated for more than 15 passages and exhibited a morphology similar to that seen in EG cells generated using bFGF alone, we further analyzed their characteristics. First, we examined expression patterns of nine genes specific for germ cells or pluripotent cells in PGCs, EG cells, and ES cells. The EG cells induced by bFGF + 2i + A83 showed gene expression profiles similar to those of EG cells cultured in the presence of bFGF alone and of ES cells, but distinct from either of the parental PGCs (Fig. 2, a–i). Microarray analysis showed highly correlated gene expression patterns between EG cells generated in the presence of bFGF + 2i + A83 compared with those without 2i + A83 (Supplemental Fig. S2). To determine the differentiation capacity of these cells, we transplanted 1×10^6 EG cells subcutaneously into nude mice and observed teratomas containing all three germ layers in EG cells generated by bFGF or by bFGF + 2i + A83 (Fig. 2j). To confirm that these EG cells originated from PGCs, we evaluated methylation patterns of imprinted loci. When differentially methylated regions of *Igf2r* and *Peg1* were analyzed by bisulfite sequence, both types of EG cells exhibited erased methylation at imprinted loci compared with mouse embryonic fibroblasts (MEFs) and TT2 ES cells (Fig. 2k). These data indicate that pluripotent cells established from E11.5 PGCs and cultured with bFGF + 2i + A83 are identical in whole-transcription and in vitro differentiation capacities.

Establishment of the Purification Method for Pluripotent Candidate Cells from PGCs

Enhanced efficiency of EG cell formation observed in the presence of bFGF + 2i + A83 led us to investigate the process of pluripotency acquisition. The PGCs were cultured with 2i + A83, bFGF, bFGF + 2i + A83, or without treatment and then monitored on Days 3 and 6 for SSEA-1 and *Nanog-GFP* double positivity (Fig. 3a). Whereas SSEA-1-positive or *Nanog-GFP*–positive cells were detected in all culture conditions at Day 3, the double-positive (DP) population was detected only in bFGF or bFGF + 2i + A83 cultures on Day 6 (Fig. 3a).

To examine whether the DP population on Days 3 and 6 included potentially pluripotent stem cells likely to form by Day 10, the DP population and the others derived in the presence of bFGF were sorted by FACS on Days 3 and 6, plated at 400 cells per well on feeder layers, and cultured. By Day 10, only cells from the DP population formed EG cell colonies, whereas cells from the non-DP population did not (Fig. 3b). Because we replated the cells, the colony formation by nascent PGC/EG cells may be included in addition to the secondary colonies. Therefore, colony formation efficiency was calculated as relative numbers. The relative colony formation efficiencies from DP populations cultured with bFGF + 2i + A83 and sorted at Days 3 and 6 of culture were 18.8% and 43.6%, respectively, whereas DP PGCs cultured with bFGF alone showed efficiencies of only 1.6% and 1.8% on Days 3 and 6, respectively. These findings indicate that culturing in the presence of bFGF + 2i + A83 enhances efficiency of EG cell formation, and combined with FACS sorting facilitates enrichment of candidate EG cells.

We also used time-lapse imaging to examine whether colonies were derived from a single cell. The DP cells were sorted on Day 3 of the culture, and then time-lapse analyses were performed for more than 70 h. This technique revealed that a single EG cell colony was not always derived from a single cell, but from the fusion of smaller colonies derived from single cells (Fig. 4, a and b, and Supplemental Movies S1 and S2). To estimate the frequency of fusion, we compared numbers of colonies formed from a single cell with those derived from bulk culture. Using single-cell deposition from sorted cells, single cells on Day 6 were cultured in the presence of bFGF + 2i + A83. These cells gave rise to EG colonies with an efficiency of 51.3%, slightly higher than that seen in bulk culture of 400 cells (43.5%; Fig. 4b). Based on these data, the frequency of fusion was calculated to be roughly 15.2%. Thus, approximately 1 colony per 6.6 colonies was generated by fusion in the bulk culture.

Cell Cycle Shifts to S Phase During Acquisition of Pluripotency

Pluripotent cells, such as ES and iPS cells, show a greater percentage of cells in S phase compared with somatic and germ stem cells [25]. Therefore, we asked whether cells in our culture system showed cell cycle progression patterns reminiscent of stem cells during pluripotency acquisition. The PGCs from an E11.5 embryo showed distinct peaks at the G_1 and G_2/M phases (G_1: 27.7%, S: 31.6%, G_2/M: 40.0%; Fig. 5b). By Day 3 of culture, almost half of those cells (49.5%) exhibited fragmented DNA (Fig. 5), indicative of cell death. Interestingly, 2i + A83 treatment in the presence of bFGF suppressed cell death to 29.0% at that time point. On Day 6, the dead cell population was drastically reduced with or without 2i + A83 treatment, and the cell cycle pattern was similar to that of established EG cells grown in either bFGF or bFGF + 2i + A83 culture conditions. These data indicate that cell death is induced at early phases of EG cell formation and that a positive effect of bFGF + 2i + A83 on cell survival may underlie the observed increase in frequency of EG cell formation.

Purified Pluripotent Candidate Cells Undergo Changes in Gene Expression

To identify pathways responsible for pluripotency acquisition, pluripotent candidate populations cultured with 2i + A83 were sorted on Days 3 and 6. The expression levels of genes were analyzed by microarray. The coefficients of correlation between all periods of culture cells were calculated and summarized in Figure 6a. From E11.5 PGCs to EG cells, the coefficients of correlation were monotonically decreased. Therefore, it is indicated that the change in gene expression was a gradual process. Principal component analysis also showed gradual changes of cell state (Fig. 6b).

To further resolve these temporal changes, we made unsupervised hierarchical clustering (Fig. 6c). The cells were divided to two clusters between Days 3 and 6 of the culture. From Day 3 to Day 6 of the culture, dead cells were decreased, and the cell cycle progression was observed (Fig. 5). Clustering analysis indicated that the transition also occurred on a transcriptional level. Interestingly, the up-regulation of *Myc*, which regulated cell survival and proliferation, was observed on Day 6 of the culture (Supplemental Table S1). Furthermore, the clustering data revealed the specific clustered genes at each

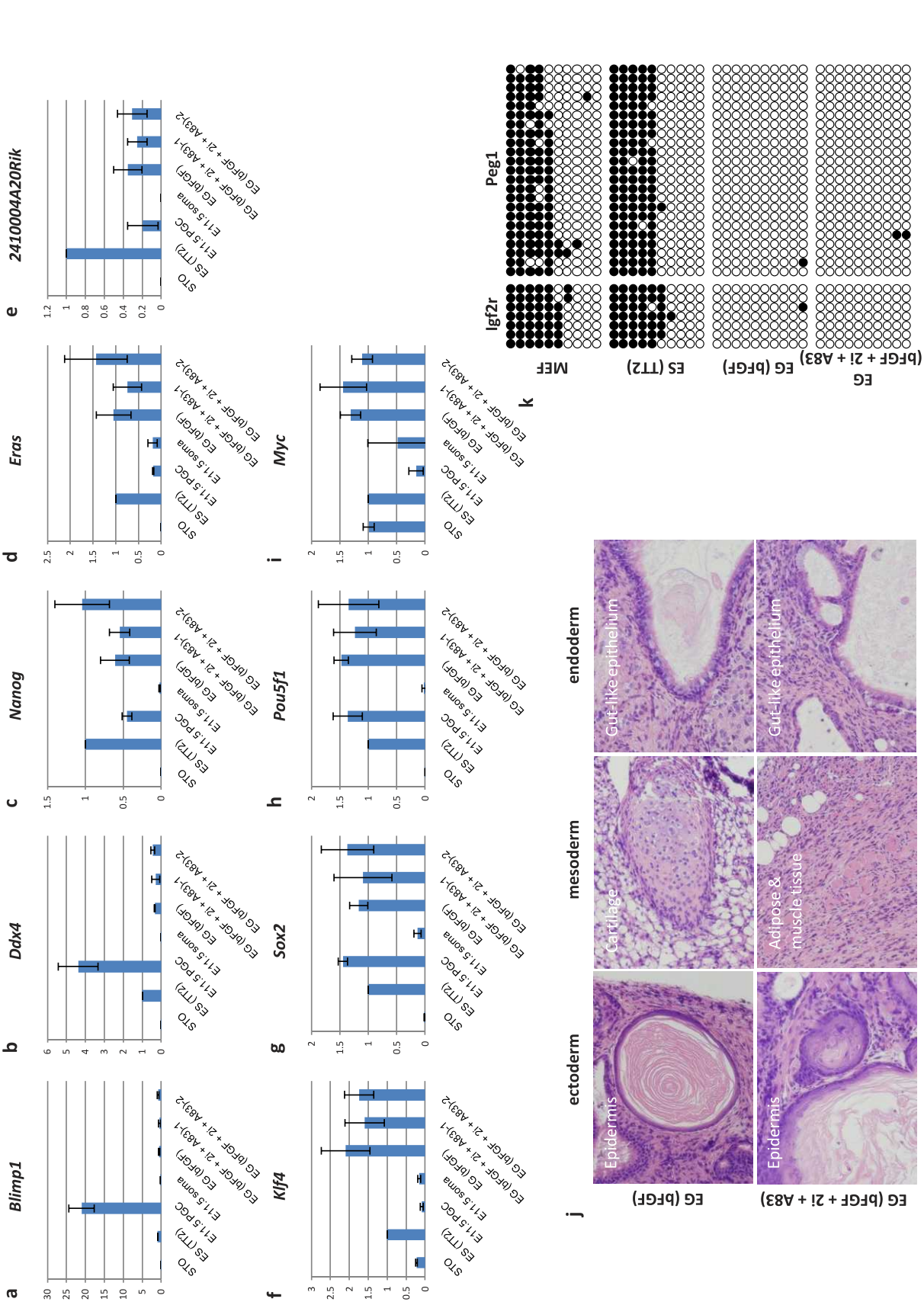

FIG. 2. Characteristics of 2i + A83-treated EG cells. Gene expression patterns were studied in the following cells. EG (bFGF + 2i + A83)-1 and –2; induced EG cells supported by bFGF + 2i + A83; EG (bFGF): induced EG cells supported by FGF alone; ES (TT2), E11.5 PGC: parental PGC; E11.5 soma: somatic cells; and STO cells. Germ cell markers: *Blimp1* (**a**) and *Ddx4* (**b**). Pluripotent cell markers: *Nanog* (**c**), *Eras* (**d**), and *2410004A20Rik* (ECAT1: **e**). Known reprogramming factors: *Klf4* (**f**), *Sox2* (**g**), *Pou5f1* (**h**), and *Myc* (**i**). The data showed relative gene expression levels. Error bars indicate SD. **j** In vivo differentiation capacity of bFGF + 2i + A83-treated EG cells or bFGF-treated EG cells. Teratoma formation from EG cells generated by each culture showed equivalent differentiation capacity. Original magnification ×10. **k** Bisulfite sequencing of EG cells at the differentially methylated region (DMR) of the imprinted genes *Igf2r* and *Peg1*. White circles indicate unmethylated CpG dinucleotides, whereas black circles indicate methylated CpG dinucleotides. The methylation pattern in EG cells (bFGF + Ti; bFGF) was different from that of MEFs and ES cells (TT2).

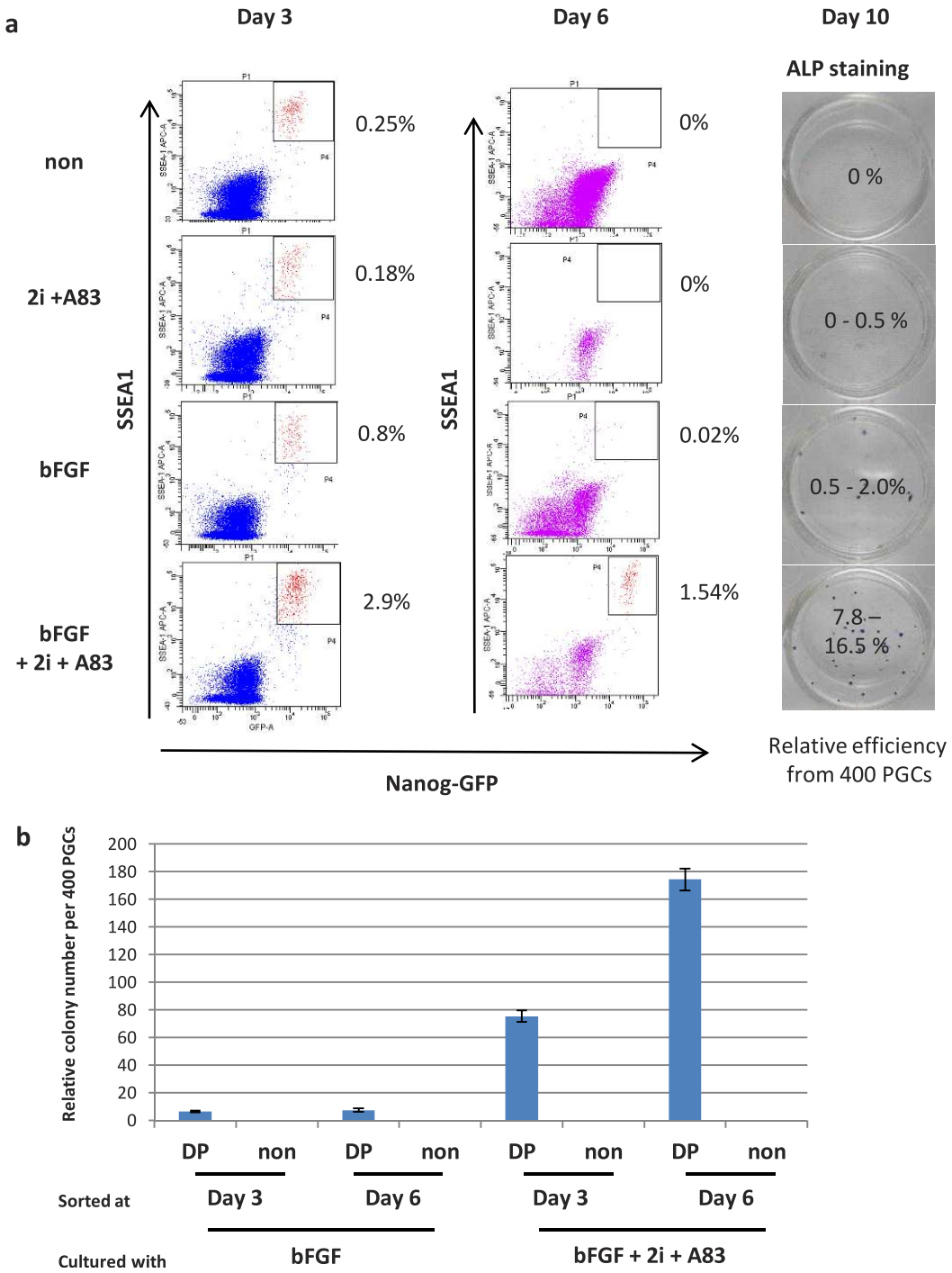

FIG. 3. Tracing PGC conversion to EG cells. **a**) *Nanog-GFP*-positive and SSEA1-positive cells were detected by FACS during EG cell formation from PGCs. Double-positive (DP) cells were analyzed on Culture Days 3 and 6 under each condition. Data representing the average percentage of DP cells from five independent experiments are displayed. At right, EG colonies on Culture Day 10 were visualized by alkaline phosphatase (ALP) staining, and colony formation efficiencies are shown. **b**) Numbers of *Nanog-GFP*-positive colonies from sorted DP and non-DP cells on Days 3 and 6. All of the culture conditions contained LIF. Error bars indicate SD.

time point. Before culture, E11.5 PGCs expressed germ cell-specific genes, such as *Dnd1* and *Ddx4*. On Day 3, the early phase of culture, some ES cell-associated genes, such as *Klf4* and *Eras*, started to become up-regulated (pluripotent cell marker; Supplemental Table S2). At that time, the expression of the germ cell markers *Dnd1* and *Ddx4* started to decrease (germ cell marker; Supplemental Table S2). On Day 6, a further decrease was observed in the expression of germ cell-characteristic genes.

To find cell fate transition from germ lineage to pluripotency on the whole-transcription level, we did enrichment plot analysis (Fig. 6, d and e). Analyzed makers were listed in Supplemental Table S2. According to the culture periods, germ cell markers decreased ($P = 0.01$) and pluripotency markers increased ($P = 0.005$) in whole transcriptome. These data suggest the cell fate transition from the transcriptome level. Recently, it has been reported that mesenchymal-to-epithelial transition is a characteristic event in the early phase of iPS cell

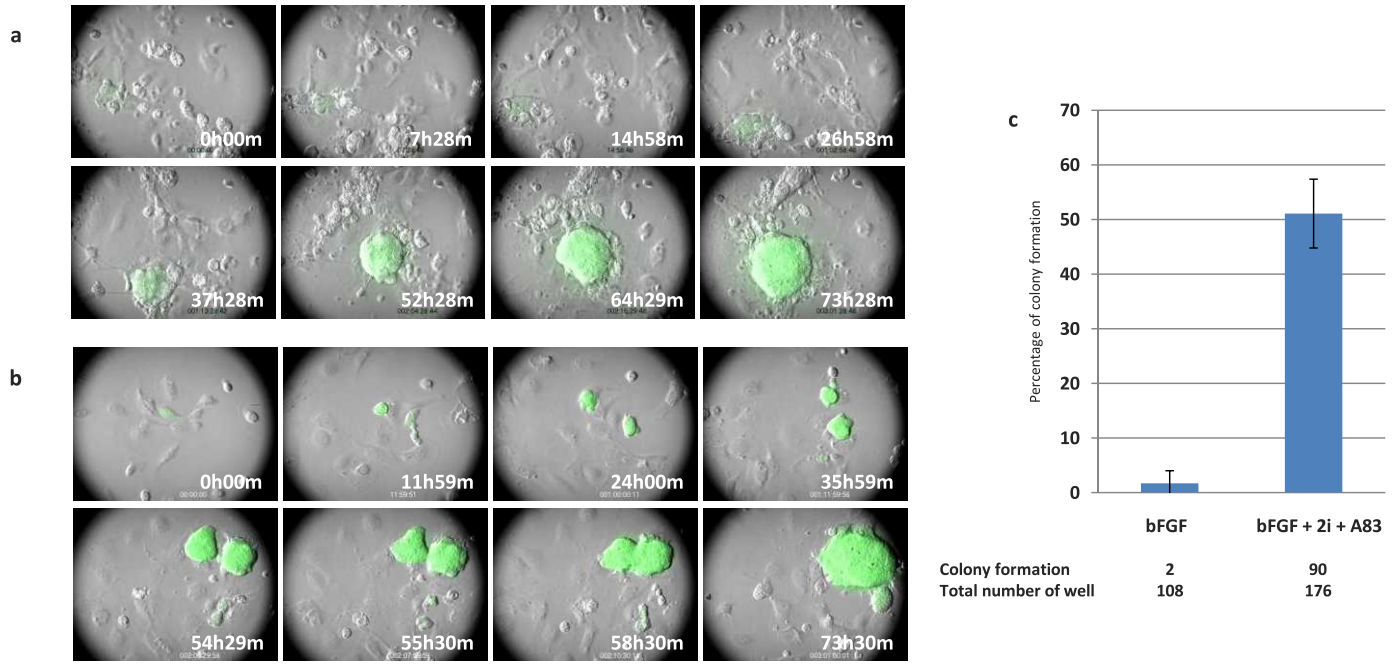

FIG. 4. Time-lapse analysis of EG cell formation. **a** and **b**) A single cell sorted from PGCs cultured with bFGF and 2i + A83 on Day 6 was traced by time-lapse imaging analysis. **a**) Formation of a single cell-derived colony (Supplemental Movie S1). **b**) Formation of a colony by cell fusion (Supplemental Movie S2). Original magnification ×20. **c**) Single DP cells supported by bFGF or bFGF + 2i + A83 were sorted into individual wells of 96-well plates on Day 6. The conversion efficiency is shown as the percentage of colony formation. All of the culture conditions contained LIF. Error bars indicate SD.

formation from fibroblasts [26]. However, our microarray data did not reveal a marked increase in epithelial gene expression (epithelial cell marker and mesenchymal cell marker; Supplemental Table S2). This might be due to the fact that PGCs avoid epithelial-to-mesenchymal transition during specification [27].

DISCUSSION

Low conversion efficiency and long culture periods have hampered the investigation of iPS cell formation from somatic cells. To overcome these experimental difficulties, we focused on the process of conversion of PGCs to pluripotent stem cells. In this study, we established more effective conditions for induction by screening different chemical compounds and purifying pluripotent candidate cells during EG cell formation using FACS. This system facilitated the analysis of cell cycle state and dynamic changes in gene expression.

Establishment of Highly Efficient Induction of Pluripotent Stem Cells

We analyzed various factors known to increase efficiency of nuclear transfer and/or iPS cell induction. Contrary to our expectations, epigenetic modifiers did not alter EG cell generation from PGCs. Although all of the chromatin-remodeling compounds tested are known to induce a relaxed chromatin state, PGCs reportedly already have a relatively loose chromatin structure compared with somatic cells [28], which may explain why chromatin modifiers were ineffective. Although TSA can reportedly replace bFGF signaling during EG cell formation [29], in our hands TSA did not have a positive effect on the presence of bFGF. However, MEK inhibitors did have a positive effect on PGC conversion, suggesting that the MAPK pathway functions in the induction of growth arrest and cell death during conversion. GSK3B inhibition is also known to induce the growth of many cell types, especially certain stem cell populations [30, 31], whereas aberrant activation of WNT/β-catenin signaling delays cell cycle progression of PGCs in vivo [32]. TGFB signaling in PGCs suppresses growth but supports cell migration [33]. In this study, inhibition of TGFB signaling also induced cell growth, but only in the presence of MAP2K and GSK3B inhibitors, indicating that TGFB has independent signaling functions in PGCs. Cell cycle progression is a potential risk for genetic mutation, and germ cells in particular should avoid mutation for the creation of the next generation. It could be possible that forced cell cycle progression induces cell death in PGCs. In this context, the inhibitors for cell cycle progression may promote EG cell formation. Actually, we found the inhibitors suppressed cell death at Day 3 of the culture (Fig. 5).

Establishment of the Purification Method for Pluripotent Candidate Cells from PGCs

It was previously reported that bFGF is required for the first 24 h of culture during EG cell formation [24]. The major pathways requiring bFGF are the MAPK and PIK3 signaling pathways, and activation of AKT, a serine/threonine kinase, enhances EG cell formation downstream of PIK3 [34]. Recently, it was reported that EG cells can be generated using LIF and 2i [35]. That study employed PGCs from embryos at E8.5, at which time point the efficiency of EG cell formation is higher [36]. Although our culture medium contained KSR, which may contain TGFB/activin activity, the enhancement effect of 2i + A83 was also seen in E8.5 PGCs (Supplemental Fig. S3). By contrast, culture conditions using LIF and 2i without bFGF did not generate EG cells from E11.5 PGCs (Supplemental Fig. S4). These data indicate that different signals are required for derivation of EG cells from PGCs at different developmental stages. Actually, from E8.5 to E11.5,

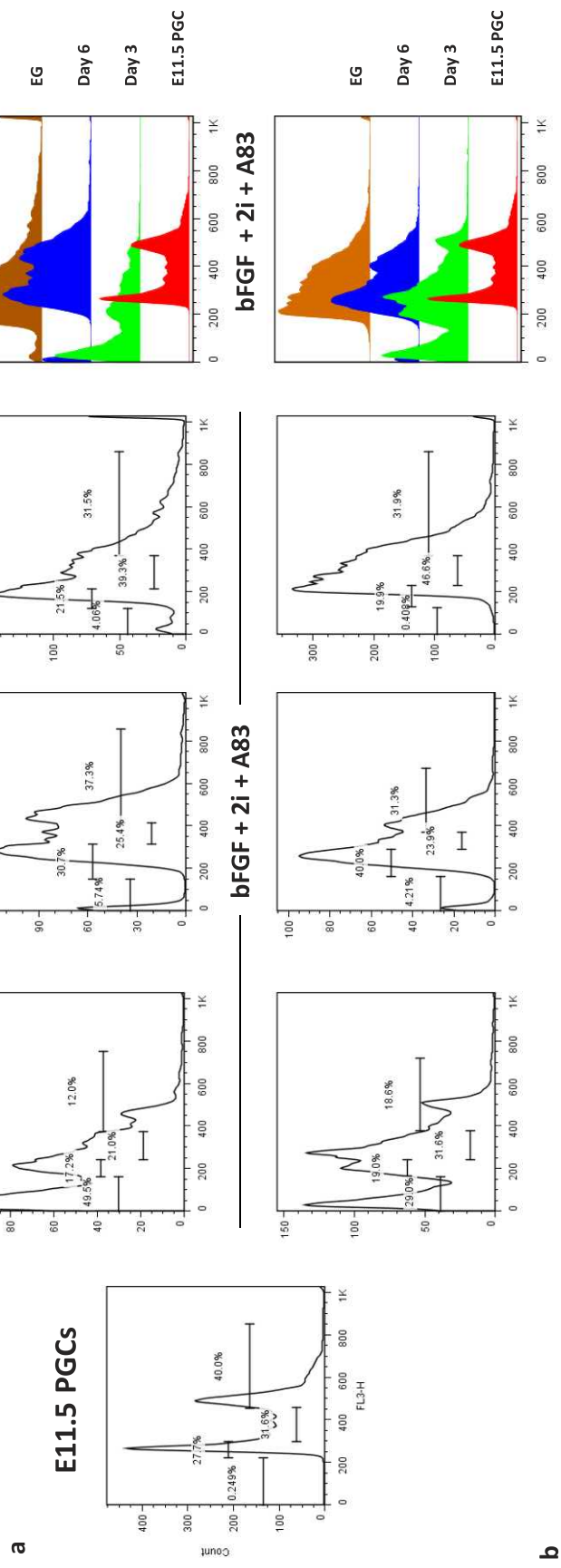

FIG. 5. Cell cycle analysis of DP cells on Days 3 and 6 of culture in the presence of bFGF or bFGF + 2i + A83 during conversion of E11.5 PGCs to EG cells. The cell cycles of E11.5 PGCs and EG cells are also shown. Histograms show DNA content as estimated by propidium iodide staining at indicated time points and culture conditions (**a**). Based on the gates indicated in the histograms above, percentages of cells at each stage of the cell cycle are shown (**b**). All of the culture conditions contained LIF.

a

CCM	E11.5PGCs	Day 3 (2i + A83)	Day 6 (2i + A83)	EG (2i + A83)
E11.5PGCs	1.00000	0.96534	0.94383	0.93126
Day 3 (2i + A83)	0.96534	1.00000	0.97616	0.95945
Day 6 (2i + A83)	0.94383	0.97616	1.00000	0.96814
EG	0.93126	0.95945	0.96814	1.00000

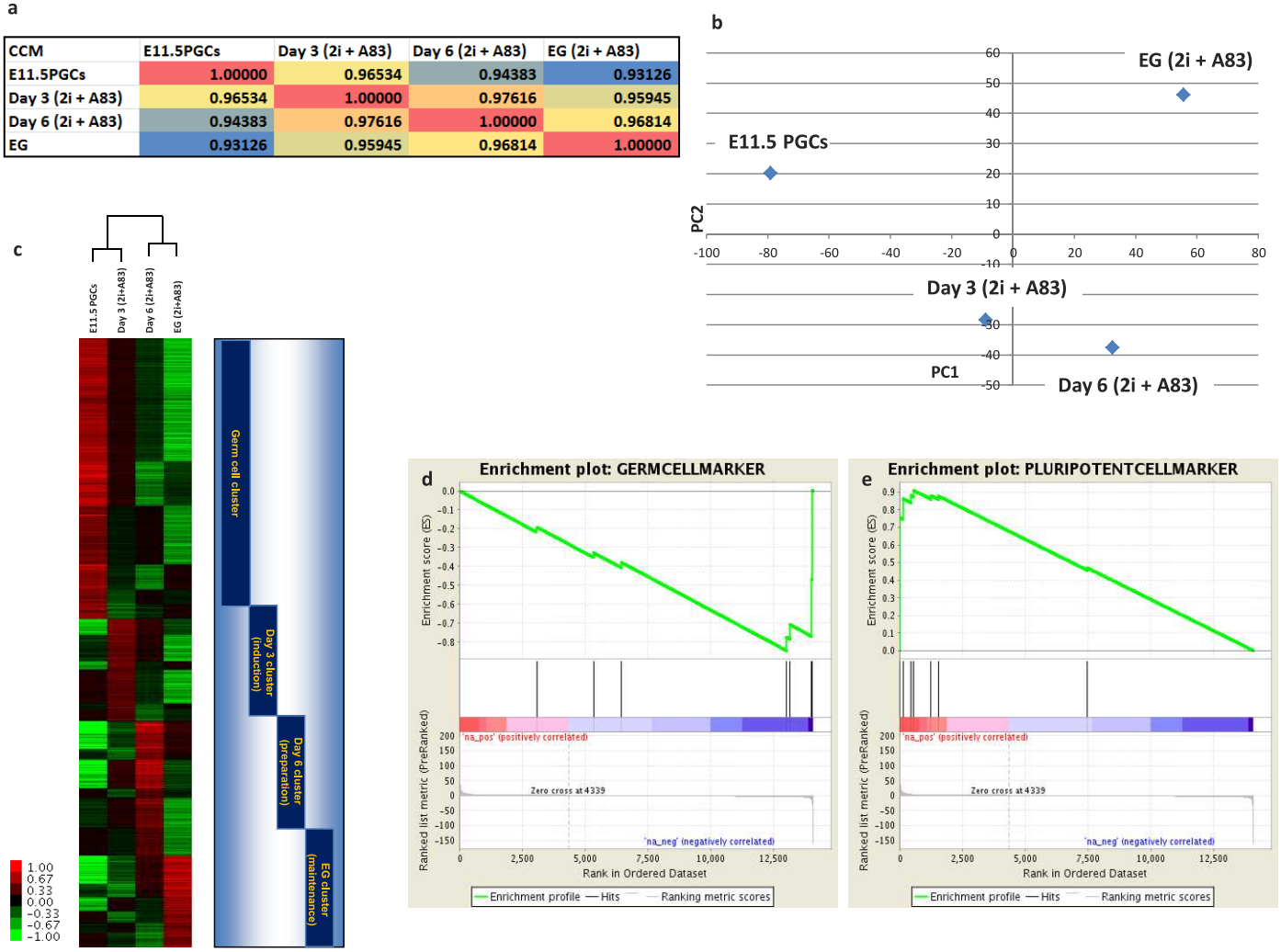

FIG. 6. Microarray analysis during EG cell formation. **a**) The coefficients of correlation between all periods of culture cells. **b**) Principal component analysis during EG cell formation. **c**) Cluster analysis of each time point. **d**) Enrichment plot analysis of germ cell markers ($P = 0.01$). **e**) Enrichment plot analysis of pluripotent cell markers ($P = 0.005$). All of the culture conditions contained LIF.

numerous events occur in PGCs, such as G_2 arrest, repression of RNA polymerase II, and environmental changes.

Pluripotent Candidate Cells Progress S Phase of Cell Cycle and Change Gene Expression Patterns During Acquisition of Pluripotency

PGCs cultured in the presence of bFGF + 2i + A83 showed highly efficient (12.1%) conversion to EG cells. When PGCs were sorted based on *Nanog* and SSEA-1 expression at Days 3 and 6 of culture, only DP cells generated pluripotent EG cells. Therefore, the 2i + A83 culture method established here clearly enhanced the efficiency of EG cell formation, and FACS facilitated purification of candidate pluripotent cells. Although technologies enabling gene expression analysis from single cells are under development, it is necessary to stringently purify candidate cells in order to accurately trace the acquisition of pluripotency.

Interestingly, cell cycle analyses indicated that many PGCs die after induction of pluripotency. The effect of 2i + A83 treatment suppressed cell death rather than the cell cycle progression (Fig. 5). The relationship between cell death and acquisition of pluripotency also indicates the presence of a subpopulation of PGCs. Primordial germ cells can reportedly be subdivided into two populations based on expression levels of the cell-surface antigen α6-integrin: cells with negative or low α6-integrin levels are likely to form EG cells, whereas high α6-integrin expressors tend to be apoptotic [37]. The fact that 2i + A83 treatment does not promote colony production from E11.5 PGCs in the absence of bFGF (Supplemental Fig. S4) suggests that treatment acts to enhance candidate EG cell survival rather than trigger acquisition of pluripotency.

Using the 2i + A83 culture and purification method, we performed gene expression analyses during the acquisition of pluripotency (Fig. 6). It has been reported that transcriptome characteristics of PGCs are different from those of pluripotent cells [38]. Our microarray data uncovered the sequential changes in transcription during the conversion of PGCs to pluripotent cells. During the acquisition of pluripotency, the loss of the original characteristics of germ cells along with the enhancement of pluripotency-associated gene expression was noted. In other words, there were at least induction, preparation, and maintenance phases during EG cell formation. This phase process is comparable to a previous microarray analysis of second iPS cell generation [26]. These results

indicate the existence of a common mechanism underlying the acquisition of pluripotency.

Considering important genes involved in the generation of EG cells from PGCs, we focused on Day 6 of the culture and gradually up-regulated genes. At Day 6 of the culture, some pluripotency markers, such as *Nanog*, *Klf4* and *Zfp42*, were expressed at their highest level during the cultures. Interestingly, at that time the *Meis* family of transcription factors also reached its highest expression (*Meis1* and *Meis2* in Supplemental Table S1). *Meis1* is known to work to maintain hematopoietic stem cells [39]. On the other hand, in the gradually up-regulated genes we found some family members of reprogramming factors, such as *Klf9* and *Sox11*. It is interesting to examine the effect of *Meis* family genes *Klf9* and *Sox11* during the acquisition of puripotency.

Human PGCs also convert to EG cells. Human EG cells are cultured in the presence of LIF, bFGF, and forskolin [40]. Although human EG cells do not form teratoma when injected into mice, they form embryoid body and differentiate into all three germ layers [41, 42]. In mice, EG cells are very similar to ES cells. However, in humans EG cells showed some differences from ES cells. Human EG cells are expressed SSEA-1, whereas human ES cells are not [42]. Although human EG cells are dome-shaped like mouse ES colonies, human ES cells are flat-shaped, which resembles mouse epiblast stem cells [40]. To understand the differences between EG cells and ES cells among species, our microarray data and culture system would provide useful information.

ACKNOWLEDGMENT

We thank Drs. H. Okano, S. Nishiyama, and W. Akamatsu (Keio University) for providing the inhibitors PD173074, PD325901, and CHIR99021, and Drs. J.-W. Cheong and A. Ishizu for critical reading of the manuscript.

REFERENCES

1. Takahashi K, Yamanaka S. Induction of pluripotent stem cells from mouse embryonic and adult fibroblast cultures by defined factors. Cell 2006; 126: 663–676.
2. Takahashi K, Tanabe K, Ohnuki M, Narita M, Ichisaka T, Tomoda K, Yamanaka S. Induction of pluripotent stem cells from adult human fibroblasts by defined factors. Cell 2007; 131:861–872.
3. Park IH, Arora N, Huo H, Maherali N, Ahfeldt T, Shimamura A, Lensch MW, Cowan C, Hochedlinger K, Daley GQ. Disease-specific induced pluripotent stem cells. Cell 2008; 134:877–886.
4. Dimos JT, Rodolfa KT, Niakan KK, Weisenthal LM, Mitsumoto H, Chung W, Croft GF, Saphier G, Leibel R, Goland R, Wichterle H, Henderson CE, et al. Induced pluripotent stem cells generated from patients with ALS can be differentiated into motor neurons. Science 2008; 321:1218–1221.
5. Ebert AD, Yu J, Rose FF Jr., Mattis VB, Lorson CL, Thomson JA, Svendsen CN. Induced pluripotent stem cells from a spinal muscular atrophy patient. Nature 2009; 457:277–280.
6. Lee G, Papapetrou EP, Kim H, Chambers SM, Tomishima MJ, Fasano CA, Ganat YM, Menon J, Shimizu F, Viale A, Tabar V, Sadelain M, et al. Modelling pathogenesis and treatment of familial dysautonomia using patient-specific iPSCs. Nature 2009; 461:402–406.
7. Okita K, Nakagawa M, Hyenjong H, Ichisaka T, Yamanaka S. Generation of mouse induced pluripotent stem cells without viral vectors. Science 2008; 322:949–953.
8. Woltjen K, Michael IP, Mohseni P, Desai R, Mileikovsky M, Hamalainen R, Cowling R, Wang W, Liu P, Gertsenstein M, Kaji K, Sung HK, et al. piggyBac transposition reprograms fibroblasts to induced pluripotent stem cells. Nature 2009; 458:766–770.
9. Zhou H, Wu S, Joo JY, Zhu S, Han DW, Lin T, Trauger S, Bien G, Yao S, Zhu Y, Siuzdak G, Scholer HR, et al. Generation of induced pluripotent stem cells using recombinant proteins. Cell Stem Cell 2009; 4:381–384.
10. Yamanaka S. Elite and stochastic models for induced pluripotent stem cell generation. Nature 2009; 460:49–52.
11. Sasaki H, Matsui Y. Epigenetic events in mammalian germ-cell development: reprogramming and beyond. Nat Rev Genet 2008; 9: 129–140.
12. Saitou M. Germ cell specification in mice. Curr Opin Genet Dev 2009; 19: 386–395.
13. Nagamatsu G, Kosaka T, Kawasumi M, Kinoshita T, Takubo K, Akiyama H, Sudo T, Kobayashi T, Oya M, Suda T. A germ cell specific gene, Prmt5 works as somatic cell reprogramming. J Biol Chem 2011; 286: 10641–10648.
14. Matsui Y, Zsebo K, Hogan BL. Derivation of pluripotential embryonic stem cells from murine primordial germ cells in culture. Cell 1992; 70: 841–847.
15. Kanatsu-Shinohara M, Inoue K, Lee J, Yoshimoto M, Ogonuki N, Miki H, Baba S, Kato T, Kazuki Y, Toyokuni S, Toyoshima M, Niwa O, et al. Generation of pluripotent stem cells from neonatal mouse testis. Cell 2004; 119:1001–1012.
16. Lucifero D, Mertineit C, Clarke HJ, Bestor TH, Trasler JM. Methylation dynamics of imprinted genes in mouse germ cells. Genomics 2002; 79: 530–538.
17. Okita K, Ichisaka T, Yamanaka S. Generation of germline-competent induced pluripotent stem cells. Nature 2007; 448:313–317.
18. Kishigami S, Mizutani E, Ohta H, Hikichi T, Thuan NV, Wakayama S, Bui HT, Wakayama T. Significant improvement of mouse cloning technique by treatment with trichostatin A after somatic nuclear transfer. Biochem Biophys Res Commun 2006; 340:183–189.
19. Huangfu D, Maehr R, Guo W, Eijkelenboom A, Snitow M, Chen AE, Melton DA. Induction of pluripotent stem cells by defined factors is greatly improved by small-molecule compounds. Nat Biotechnol 2008; 26:795–797.
20. Blelloch R, Wang Z, Meissner A, Pollard S, Smith A, Jaenisch R. Reprogramming efficiency following somatic cell nuclear transfer is influenced by the differentiation and methylation state of the donor nucleus. Stem Cells 2006; 24:2007–2013.
21. Li W, Wei W, Zhu S, Zhu J, Shi Y, Lin T, Hao E, Hayek A, Deng H, Ding S. Generation of rat and human induced pluripotent stem cells by combining genetic reprogramming and chemical inhibitors. Cell Stem Cell 2009; 4:16–19.
22. Ying QL, Wray J, Nichols J, Batlle-Morera L, Doble B, Woodgett J, Cohen P, Smith A. The ground state of embryonic stem cell self-renewal. Nature 2008; 453:519–523.
23. Silva J, Barrandon O, Nichols J, Kawaguchi J, Theunissen TW, Smith A. Promotion of reprogramming to ground state pluripotency by signal inhibition. PLoS Biol 2008; 6:e253.
24. Durcova-Hills G, Adams IR, Barton SC, Surani MA, McLaren A. The role of exogenous fibroblast growth factor-2 on the reprogramming of primordial germ cells into pluripotent stem cells. Stem Cells 2006; 24: 1441–1449.
25. Fujii-Yamamoto H, Kim JM, Arai K, Masai H. Cell cycle and developmental regulations of replication factors in mouse embryonic stem cells. J Biol Chem 2005; 280:12976–12987.
26. Samavarchi-Tehrani P, Golipour A, David L, Sung HK, Beyer TA, Datti A, Woltjen K, Nagy A, Wrana JL. Functional genomics reveals a BMP-driven mesenchymal-to-epithelial transition in the initiation of somatic cell reprogramming. Cell Stem Cell 2010; 7:64–77.
27. Kurimoto K, Yabuta Y, Ohinata Y, Shigeta M, Yamanaka K, Saitou M. Complex genome-wide transcription dynamics orchestrated by Blimp1 for the specification of the germ cell lineage in mice. Genes Dev 2008; 22: 1617–1635.
28. Seki Y, Yamaji M, Yabuta Y, Sano M, Shigeta M, Matsui Y, Saga Y, Tachibana M, Shinkai Y, Saitou M. Cellular dynamics associated with the genome-wide epigenetic reprogramming in migrating primordial germ cells in mice. Development 2007; 134:2627–2638.
29. Durcova-Hills G, Tang F, Doody G, Tooze R, Surani MA. Reprogramming primordial germ cells into pluripotent stem cells. PLoS ONE 2008; 3:e3531.
30. Zechner D, Fujita Y, Hulsken J, Muller T, Walther I, Taketo MM, Crenshaw EB, 3rd, Birchmeier W, Birchmeier C. beta-Catenin signals regulate cell growth and the balance between progenitor cell expansion and differentiation in the nervous system.Dev Biol 2003; 258:406–418.
31. Sato N, Meijer L, Skaltsounis L, Greengard P, Brivanlou AH. Maintenance of pluripotency in human and mouse embryonic stem cells through activation of Wnt signaling by a pharmacological GSK-3-specific inhibitor. Nat Med 2004; 10:55–63.
32. Kimura T, Nakamura T, Murayama K, Umehara H, Yamano N, Watanabe S, Taketo MM, Nakano T. The stabilization of beta-catenin leads to impaired primordial germ cell development via aberrant cell cycle progression. Dev Biol 2006; 300:545–553.
33. Godin I, Wylie CC. TGF beta 1 inhibits proliferation and has a

chemotropic effect on mouse primordial germ cells in culture. Development 1991; 113:1451–1457.
34. Kimura T, Tomooka M, Yamano N, Murayama K, Matoba S, Umehara H, Kanai Y, Nakano T. AKT signaling promotes derivation of embryonic germ cells from primordial germ cells. Development 2008; 135:869–879.
35. Leitch HG, Blair K, Mansfield W, Ayetey H, Humphreys P, Nichols J, Surani MA, Smith A. Embryonic germ cells from mice and rats exhibit properties consistent with a generic pluripotent ground state. Development 2010; 2010:2279–2287.
36. Labosky PA, Barlow DP, Hogan BL. Mouse embryonic germ (EG) cell lines: transmission through the germline and differences in the methylation imprint of insulin-like growth factor 2 receptor (Igf2r) gene compared with embryonic stem (ES) cell lines. Development 1994; 120:3197–3204.
37. Matsui Y, Tokitake Y. Primordial germ cells contain subpopulations that have greater ability to develop into pluripotential stem cells. Dev Growth Differ 2009; 51:657–667.
38. Mise N, Fuchikami T, Sugimoto M, Kobayakawa S, Ike F, Ogawa T, Tada T, Kanaya S, Noce T, Abe K. Differences and similarities in the developmental status of embryo-derived stem cells and primordial germ cells revealed by global expression profiling. Genes Cells 2008; 13: 863–877.
39. Hisa T, Spence SE, Rachel RA, Fujita M, Nakamura T, Ward JM, Devor-Henneman DE, Saiki Y, Kutsuna H, Tessarollo L, Jenkins NA, Copeland NG. Hematopoietic, angiogenic and eye defects in Meis1 mutant animals. EMBO J 2004; 23:450–459.
40. Shamblott MJ, Axelman J, Wang S, Bugg EM, Littlefield JW, Donovan PJ, Blumenthal PD, Huggins GR, Gearhart JD. Derivation of pluripotent stem cells from cultured human primordial germ cells. Proc Natl Acad Sci U S A 1998; 95:13726–13731.
41. Shamblott MJ, Axelman J, Littlefield JW, Blumenthal PD, Huggins GR, Cui Y, Cheng L, Gearhart JD. Human embryonic germ cell derivatives express a broad range of developmentally distinct markers and proliferate extensively in vitro. Proc Natl Acad Sci U S A 2001; 98:113–118.
42. Turnpenny L, Brickwood S, Spalluto CM, Piper K, Cameron IT, Wilson DI, Hanley NA. Derivation of human embryonic germ cells: an alternative source of pluripotent stem cells. Stem Cells 2003; 21:598–609.